

A MULTISTEP SEGMENTATION ALGORITHM FOR VESSEL EXTRACTION IN MEDICAL IMAGING

Nasser Aghazadeh¹ , Ladan Sharafyan Cigaroudy²

^{1,2}Department of Applied Mathematics, Azarbaijan Shahid Madani University
Tabriz, Iran

aghazadeh@azaruniv.ac.ir¹, sharafyan@azaruniv.ac.ir²

ABSTRACT

The main contribution of this paper is to propose an iterative procedure for tubular structure segmentation of 2D images, which combines tight frame of Curvelet transforms with a SURE technique thresholding which is based on principle obtained by minimizing Stein Unbiased Risk Estimate for denoising. This proposed algorithm is mainly based on the TFA proposal presented in [1, 9], which we use eigenvectors of Hessian matrix of image for improving this iterative part in segmenting unclear and narrow vessels and filling the gap between separate pieces of detected vessels. The experimental results are presented to demonstrate the effectiveness of the proposed model.

Keywords: *Image segmentation Curvelets medical imaging thresholding eigenvector*

1.0 INTRODUCTION

Segmentation is a useful tool with various applications in different fields such as medical diagnosis, digital system designing and spatial images. Distinguishing objects, homogeneous tissues, edges and ridges in images with mathematical tools is a branch of image processing [5]. Image segmentation is applied in medical sciences to distinguish special tissue like tumors in tomography, ridges for vessel extraction in angiography and etc. The extraction of tubular structure of vessels has fundamental role in some automated medical diagnosis.

The paper considers tubular structure segmentation that can be applied to vessel extraction. Depending on the purpose of segmentation, various algorithms have been proposed to solve the segmentation problem. Among them there are two main methods: based on edge [11] and based on the region [4], both of which are used in our algorithm. We use Curvelet which has important role in representing edges. Also we use gradient for pre-segmenting of pixels. Both of them are edge detection tools. On the other hand, the region based technique which we use are the value of intensity function and eigenvectors of Hessian matrix for the pixels belonging to a subdomain of image which has potentiality of being vessel.

At the beginning of our algorithm we compute the discrete Gradient of image for dividing pixels into two regions: one region consists of vessel pixels and the second includes the pixels in the background. In addition, we need the eigenvectors of Hessian matrix because of their similar directions in the same and near region. In section 2, we explain the method of computing first and second order derivatives of the image which are used in the discrete Gradient of image and Hessian matrix. In section 3, we briefly introduce the tight frame of Curvelets transform, that we choose for decomposition and reconstruction of the image to arrange denoising part. After the image decomposition (Curvelet transform of image) and before the reconstruction (inverse of Curvelet transform), we use SURE technique thresholding [8] for denoising. In section 4, we describe this technique. In section 5, we completely illustrate our iterative algorithm step by step, all calculated parameters of previous sections are used in this part. At last, in section 6, we present four examples to show our experimental results.

2.0 GAUSSIAN GRADIENT AND EIGENVECTOR OF HESSIAN MATRIX

In the angiography images, ridges are natural indicators of vessels. Ridges are defined as points where the image has an extremum in the direction of the largest surface curvature. Thus, the first derivative of the intensity in the direction of the largest surface curvature changes sign. The interested reader can consult [19] and the references therein for a more detailed review of the surface curvature. The direction of largest surface curvature is the eigenvector \mathbf{v} of the matrix of second order derivatives of the image corresponding to the largest absolute eigenvalue λ . This matrix is referred to as the Hessian matrix \mathbf{H} for any 2D image f

$$\nabla^2 f(X) = H(X) = \begin{bmatrix} f_{xx} & f_{xy} \\ f_{yx} & f_{yy} \end{bmatrix}.$$

Taking derivatives of discrete images is an ill-posed operation [17], thus they are taken at a scale σ using the Gaussian scale-space technique [10]. The main idea is that the image derivatives can be taken by convolving the image with derivatives of a Gaussian kernel with respect to a coordinate of image such as x ,

$$\frac{\partial f(X, \sigma)}{\partial x} = \frac{1}{2\pi\sigma^2} \int_{X' \in \mathbb{R}^2} \frac{\partial}{\partial x} \frac{e^{-\frac{|X-X'|^2}{2\sigma^2}}}{2\sigma^2} f(X') dX', \quad (1)$$

where $X = (x, y)$. The derivation with respect to y is done in the same manner. Mixed and higher order derivatives are computed by taking mixed and higher order derivatives of the Gaussian kernel.

Another idea that we use in the steps of our algorithm is the fact that the directions of eigenvectors (\mathbf{v}) of the ridge pixels should be similar [11]. If the pixels have similar orientation the scalar product will be close to 1. One parameter that we calculate and use in each step is the mean value ($\text{mean}^{(i)}$) of scalar product of eigenvector \mathbf{v} of the pixel of maximum gradient with the other pixels in $\Lambda^{(i)}$ (in each step, $\Lambda^{(i)}$ includes the pixels which have potential of being vessel).

3.0 TIGHT FRAME OF CURVELETS TRANSFORM

Despite the fact that wavelets have had a wide impact in image processing (see [12, 13]) they fail to efficiently represent objects with highly anisotropic elements such as lines or curvilinear structures (e.g. edges). The reason is that wavelets are non-geometrical and do not exploit the regularity of the edge curve. The Ridgelet and the Curvelet transforms were developed as an answer to the weakness of the separable wavelet transform in sparsely representing of what appears to be simple building atoms in an image, e.g. lines, curves and edges. Curvelets and Ridgelets take the form of basis elements which exhibit high directional sensitivity and are highly anisotropic [6, 7]. Ridgelets and Curvelets are special members of the family of multiscale orientation-selective transforms, which have recently led to a flurry of research activity in the field of computational and applied harmonic analysis. Curvelet transform developed by Candes and Donoho is a multiscale transform designed to represent edges and other singularities along curves much more efficiently than the traditional transforms, i.e., using fewer coefficients for a given accuracy of reconstruction [8].

In this paper, we use Fast Discrete Curvelet Transforms from [18]. This transformation is based on unequally-spaced fast Fourier transforms (USFFT). This implementation is fast in the sense that it runs in $O(n^2 \log n)$ flops for n by n Cartesian arrays; in addition, it is invertible, with rapid inversion algorithms of about the same complexity. We use MATLAB based CurveLab toolbox and the software CurveLab, which implement this transform from [18].

If we introduce $\mathcal{C}(\cdot)$ as Curvelet transform (decomposition) operator, T_λ (see section 3) as thresholding operator and $\mathcal{IC}(\cdot)$ as inverse Curvelet transform (reconstruction) operator, then we use

$$\mathcal{IC}(T_\lambda(\mathcal{C}(f^{(i)}))) \quad (2)$$

for denoising $f^{(i)}$ in each step. It is noticeable that we have $\mathcal{IC}(\mathcal{C}(f)) = f$, because we use tight frame Curvelets [14, 3].

4.0 Thresholding

We use a thresholding technique based on a principle derived by minimizing Stein Unbiased Risk Estimate (SURE)[8]. A standard application of SURE is to choose a parametric form for an estimator, and then optimize the values of the parameters to minimize the risk estimate. This technique has been applied in several settings. It has been used by Donoho and Johnstone to determine the optimal shrinkage factor in a wavelet denoising setting [16]. We use this technique for estimate the hard thresholding parameter for denoising based on Curvelet as follow.

We change $Nx \times Ny$ matrix of image f into vector F with size $Nxy = Nx * Ny$ and sort its second powers:

$$a = \text{sort}\{|F_j|^2\}_{j=1}^{Nxy},$$

and calculate other parameters:

$$b = \{\sum_{r=1}^j a_r\}_{j=1}^{Nxy},$$

$$c = \{Nxy - j\}_{j=1}^{Nxy},$$

$$s = \{b_j + c_j a_j\}_{j=1}^{Nxy},$$

$$risk = \left\{ \frac{n-2j+s_j}{n} \right\}_{j=1}^{Nxy},$$

then let

$$risk_{best} = \min \{risk_j\}_{j=1}^{Nxy},$$

and

$$\lambda_{thresh} = \sqrt{a_{best}}.$$

We use λ_{thresh} for image hard thresholding.

5.0 THE ITERATIVE ALGORITHM

The main idea of this algorithm is based on TFA [1, 2]. We explain the algorithm with more details that we have added to it. At first, we define $f^{(i)} \equiv f$ for $i = 0$ and

$$\Lambda^{(i)} \equiv \{(x, y) \in \Omega \mid \|\nabla f(x, y)\|_2 \geq \varepsilon\}, \quad (3)$$

for a small supposed ε . Here $\nabla f(x, y)$ is the discrete gradient of f at the pixel (x, y) that we compute with Gaussian scale-space technique. Now we continue the iterative process with the initial data Λ^0 and f^0 .

STEP1: We compute the maximum gradient and find the pixel with maximum gradient

$$maxg = \max\{\|\nabla f(x, y)\|_2 \mid (x, y) \in \Lambda^{(i)}\} = \|\nabla f(x, y)\|_2, \quad (\bar{x}, \bar{y}) \in \Lambda^{(i)} \quad (4)$$

$$maxp = (\bar{x}, \bar{y}). \quad (5)$$

STEP2: Compute four decision parameters, $mean^{(i)}, M^{(i)}, Mn^{(i)}$ and $Mp^{(i)}$:

$$mean^{(i)} = \frac{\sum_{(x,y) \in \Lambda^{(i)}} \nabla f(x,y)}{|\Lambda^{(i)}|}, \quad (6)$$

and

$$M^{(i)} = \frac{\sum_{(x,y) \in \Lambda^{(i)}} f^{(i)}(x,y)}{|\Lambda^{(i)}|}, \quad (7)$$

and

$$M_p^{(i)} = \frac{\sum_{\{(x,y) \in \Lambda^{(i)} \mid f^{(i)}(x,y) \geq M^{(i)}\}} f^{(i)}(x,y)}{|\{(x,y) \in \Lambda^{(i)} \mid f^{(i)}(x,y) \geq M^{(i)}\}|}, \quad (8)$$

and

$$M_n^{(i)} = \frac{\sum_{\{(x,y) \in \Lambda^{(i)} \mid f^{(i)}(x,y) \leq m^{(i)}\}} f^{(i)}(x,y)}{|\{(x,y) \in \Lambda^{(i)} \mid f^{(i)}(x,y) \leq m^{(i)}\}|}. \quad (9)$$

We define

$$\alpha_i \equiv \max\{\frac{M^{(i)} + M_p^{(i)}}{2}, 0\}, \quad \beta_i \equiv \min\{\frac{M^{(i)} + M_p^{(i)}}{2}, 1\}. \quad (10)$$

The main difference of our algorithm and TFA in this step is equation (6).

STEP3: Image can be thresholded by introducing the $f_t^{(i)}$ which subdivide the image into three parts:

$$f_t^{(i)}(x,y) = \begin{cases} 0 & f^{(i)}(x,y) \leq \alpha_i \\ 1 & \text{if } \{f^{(i)}(x,y) \geq M^{(i)} \text{ and } v(max_p), v(x,y) \geq mean^{(i)}\} \\ & \text{or } f^{(i)}(x,y) \geq \beta_i \\ \frac{f^{(i)}(x,y) - min_i}{max_i - min_i} & o.w., \end{cases} \quad (11)$$

where

$$max_i = \max\{f^{(i)}(x,y) \mid \alpha_i \leq f^{(i)}(x,y) \leq \beta_i, (x,y) \in \Lambda^{(i)}\},$$

$$min_i = \min\{f^{(i)}(x,y) \mid \alpha_i \leq f^{(i)}(x,y) \leq \beta_i, (x,y) \in \Lambda^{(i)}\}.$$

We use $mean^{(i)}$ for second constraint of $f_t^{(i)}$. The set of the remaining pixels that should be classified is denoted by:

$$\Lambda^{(i+1)} = \{(x,y) \mid 0 < f_t^{(i)}(x,y) < 1, (x,y) \in \Omega\}. \quad (12)$$

In the next step, we denoise and smooth $f_t^{(i)}$ on $\Lambda^{(i+1)}$ with Curvelets based algorithm.

STEP4 (Denoising and smoothing): In this step we apply equation (2) to $f_t^{(i)}$ on $\Lambda^{(i+1)}$ to get $f^{(i+1)}$. For the other pixels which belong to $\Omega - \Lambda^{(i+1)}$, we have $f^{(i+1)} = f_t^{(i)}$. To write it out clearly, let $F_t^{(i)} = vec(f_t^{(i)})$ where $vec(\cdot)$ represents the vector form of a two-dimensional (2D) pixel-array (size $N_x \times N_y$) by concatenation in the usual columnwise fashion, and $P^{(i+1)}$ be the diagonal matrix where the diagonal entry is 1 if the corresponding index of pixel be in $\Lambda^{(i+1)}$, and 0 otherwise. Then

$$F^{(i+1)} \equiv (I - P^{(i+1)})F_t^{(i)} + P^{(i+1)}vec(IC(T_\lambda(C(f_t^{(i)})))). \quad (13)$$

By reordering the entries of the vector $F^{(i+1)}$ into columns, we obtain the denoised and smoothed image $F^{(i+1)}$ [9]. In every iteration the cost of (13) is reduced, because it depends on the pixels of $\Lambda^{(i+1)}$, that decreases in each iteration. When $\Lambda^{(i+1)} = \emptyset$, the iteration terminates, and it happens immediately after the values of $f_t^{(i)}$ are just 1 and 0. The pixels with value 0 are considered as background and the pixels with value 1 constitute the vessels. Here, we summarize the algorithm:

- Input: given image f .
- Set $f^{(0)} = f$ and $\Lambda^{(0)}$ by (3).
- Do $i = 0, 1, 2, \dots$
 - Compute max_g by (4) and max_p by (5).
 - Compute $mean^{(i)}$ by (6) and $[\alpha_i, \beta_i]$ by (10).
 - Threshold $f^{(i)}$ into $f_t^{(i)}$ by (11).
 - Compute $\Lambda^{(i+1)}$ by (12).

- Stop if $\Lambda^{(i+1)} = \emptyset$, therefore $f_f^{(i)}$ is a binary image.
- Compute $f^{(i+1)}$ by $f_f^{(i)}$ by (13).
- Output: binary image $f_f^{(i)}$.

THEOREM 1.1 Our algorithm converges to a binary image within a finite number of steps.

PROOF. The proof follows the same arguments as in [1, Theorem 3.1]. Since $|\Lambda^{(i+1)}| \leq |\Lambda^{(i)}|$ and $|\Lambda^{(0)}|$ is finite, thus finite steps leads to $|\Lambda^{(i)}| = 0$ and $f_f^{(i)}$ becomes binary.

6.0 EXPERIMENTAL RESULTS

In this section, we present some medical images. We test our proposed algorithm and compare it with TFA [1, 2], and a Mamford-Shah based algorithm that Yibao Li and Junseok Kim used for biomodal image segmentation [15] (We refer to it by LK in the sequel). For the color images, we choose green channel for segmentation, because of its high contrast in edges. For simplicity, we refer to our segmentation method as TFAE (TFA with **eigenvector**). All computations are implemented in MATLAB 2011a running on an Intel Core i5 with about 16 significant decimal digits, and the codes of methods are provided by the authors, except for tight frame transform part and in our examples, we fix $\sigma = 2$, and $\epsilon = 0.02$.

EXAMPLE 1.2 (Effect of eigenvectors to reduce the number of iterations): In this example, we focus on the effect of scalar product of eigenvectors on reducing the number of iterations. We work on a small part of MRTA image with size 100×100 (figure 1). The first step result shows that there are some pixels (blue pixels) that TFAE at the first step can segment them as vessels while the TFA algorithm can not do it at that step. In spite of the fact that the computation order of our algorithm in each step is more than TFA's, TFAE reduces the number of iterations, therefore the running time of TFAE does not change significantly.

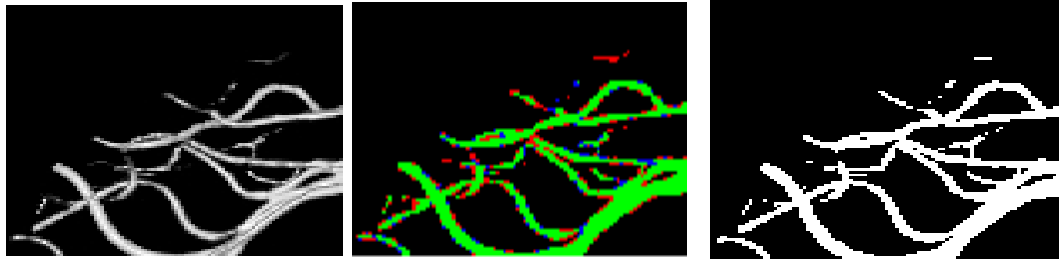


Fig. 1: True image (left), the result of the first step of TFAE (center), the blue pixels are those that TFAE distinguished them as vessels. The value of f_f in red pixels is between 0 and 1 which must be categorized into vessel or background in the next steps. The final segmented image (right)

EXAMPLE 2.3 In this example we test two angiography 216×233 and 498×500 JPEG images (figures 2) by TFAE, TFA [1, 9] and LK [15] methods. The results demonstrate that TFAE segments more unclear and narrow vessels specially in the end of vessels (the comparison between figures 2d, 2h with figures 2g, 2f and 2c), and less background pixels as a vessel (figure 2b).

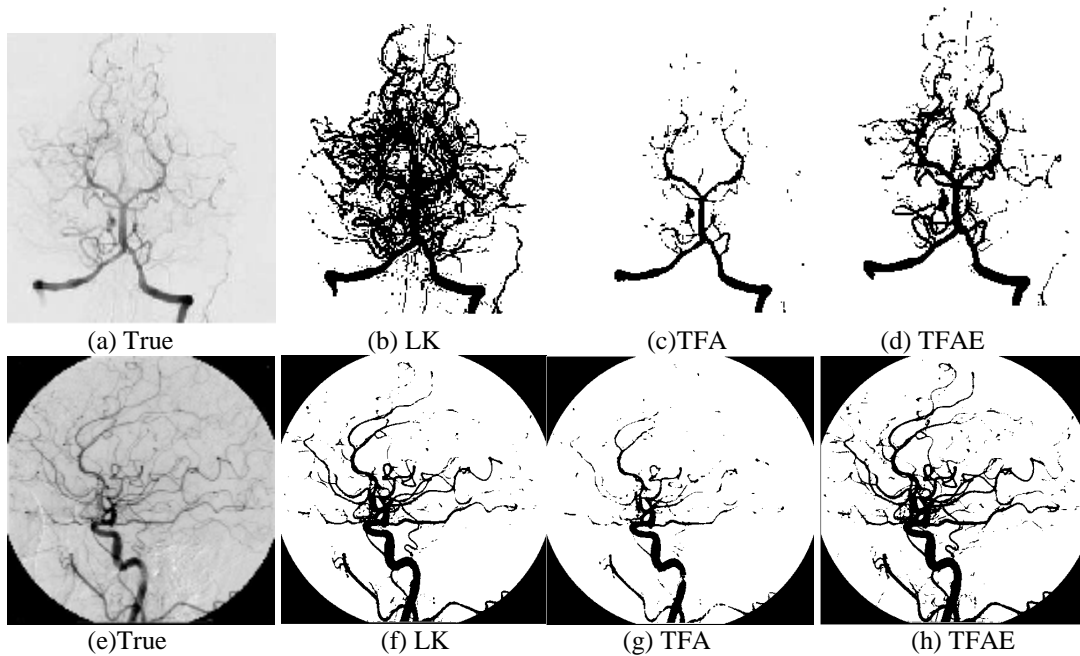


Fig. 2: True images are in the first column((a),(e)), the results of LK are in the second column ((b),(f)), the results of TFA are in the third column ((c),(g)) and the results of TFAE are in the last column ((d), (h)).

EXAMPLE 3.5 (6The dark vessel pixels) : In this example, we show that some vessel pixels with relatively dark intensity, can be distinguished as vessel by TFAE more than TFA (figure 3). In spite of difference between the intensity of this kind of pixels and other vessel pixels, the direction of their eigenvector of Hessian matrix is similar and this is the point that they can be categorized as vessel by TFAE. For this aim, we choose a 300×300 MRT Angiography image and provide the results in figure 3.

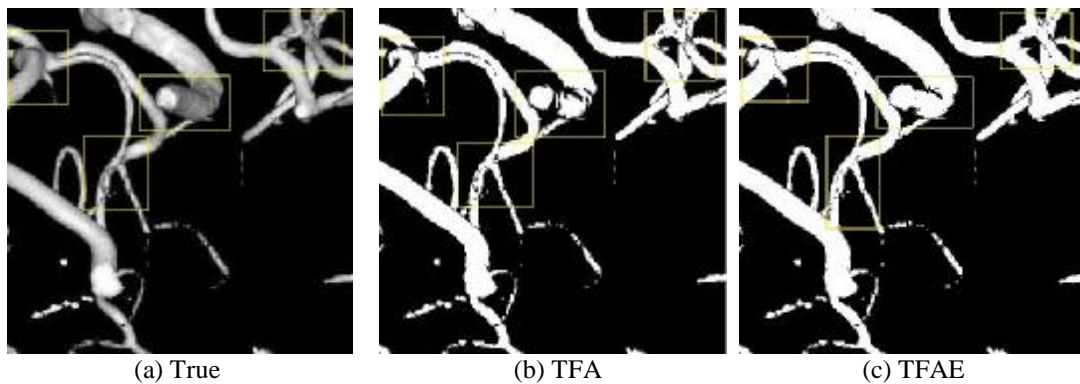


Fig. 3: (a) True image. We draw yellow rectangular boxes around the pixels in the junction of multi vessels, or in the curvature of one vessel, which have darker intensity. (b) TFA segmentation result, (c) our algorithm segmentation result.

EXAMPLE 4.7 3D time of flight MR angiography (3D-TOF-MRA) of the circle of Willis is used as an alternative to invasive radiologic procedures and other MRI methods which require the application of contrast agents. We choose three different slides of this kind of MRI images with size 512×433 and we provides the results of TFA and TFAE with the images which show different between this two results, (figure4). In the last column there are the images which show the vessele pixels which can be segmented by TFAE more than TFA (black pixels). In other word, black pixels can be

distinguished as vessel by TFAE while they can not be segmented by TFA.

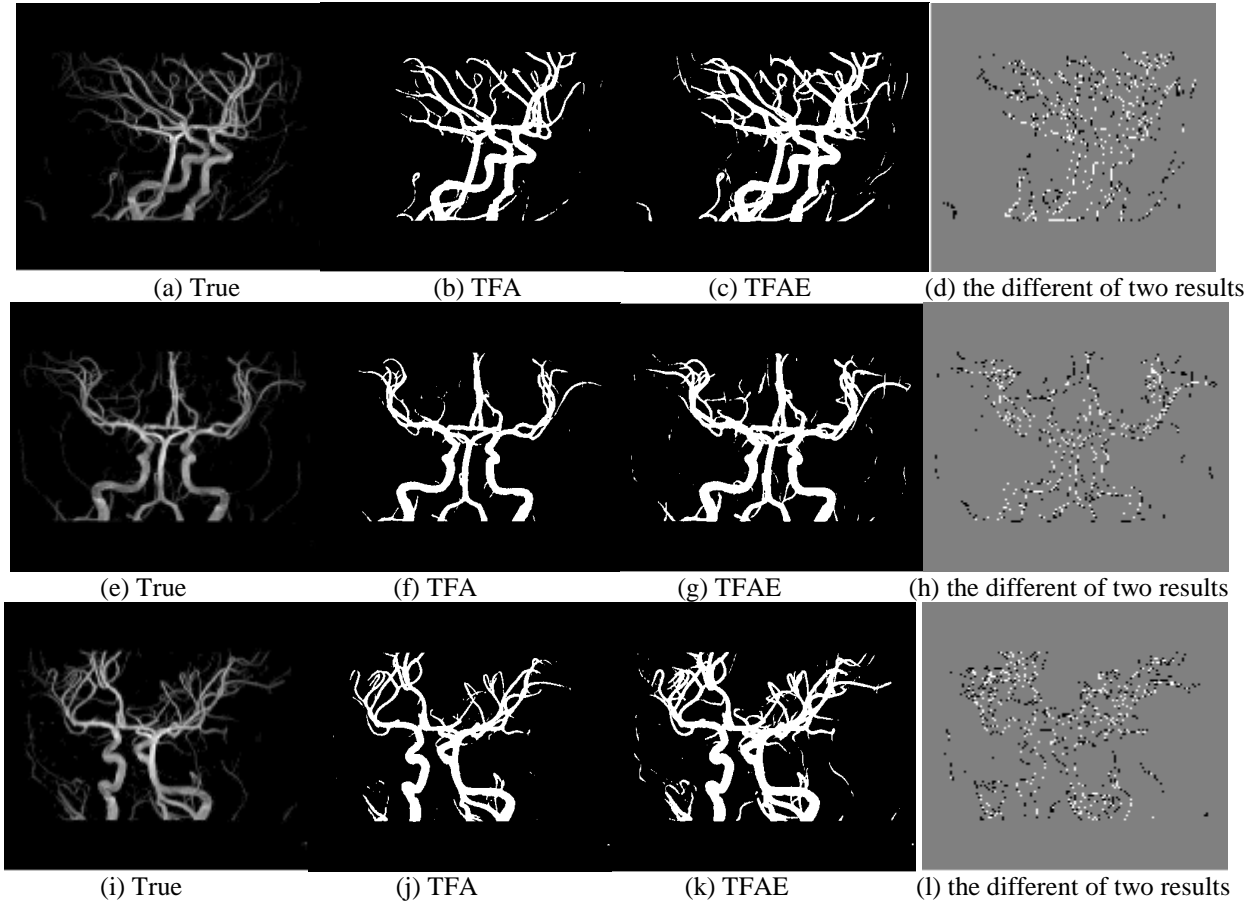


Fig. 4: True images are in the first column, results of TFA algorithm are in the second column, the results of TFAE are in the third column and the images of the forth column are the different between TFA and TFAE segmentation methods, the black pixels, which commonly belong to narrow and unclear vessels.

7.0 CONCLUSION

In this paper, with contribution of the eigenvectors of Hessian matrix and the intensity value of pixels, we have presented an algorithm for vessel extraction. The novelty stays on Stage 3 where a constraint is added to the thresholding process. A slight change in the iteration part of TFA, actually shows that in the vessel segmentation has better result. The experimental results illustrate how our algorithm does efficiently in tubular structure segmentation. Our algorithm may be further improved in several ways. We choose Curvelets because of their ability to reconstruct curves. One can choose other kind of wavelets family. Another way of improving the algorithm is to change the technique of computing image gradient into other suitable PDE formulas. We choose reasonably (as described in section 2) the Gaussian scale-space technique. Finally, we try to employ the Curvelet transform parameters as a default, one can optimize them.

REFERENCES

- [1] X. Cai, R. Chan, S. Morigi, F. Sgallari, "Vessel segmentation in medical imaging using a tight-frame based algorithm", SIAM J. Imaging, Vol. 6, No. 1, 2013, pp. 464-486.
- [2] X. Cai, R. Chan, S. Morigi, F. Sgallari, "Framelet-based algorithm for segmentation of tubular structures", Springer, Scale Space and Variational Methods in Computer Vision, Vol. 6667, 2012, pp. 411-422.
- [3] J. F. Cai, H. Jib, Z. Shen, G. B. Yea, "Data-driven tightframe construction and image denoising", Applied and Computational Harmonic Analysis, Vol. 37, 2014, pp. 89-105.
- [4] A. Sawatzky, D. Tenbrinck, X. Jiang, M. Burger, "A variational framework for regionbased segmentation incorporating physical noise model", Springer, J. Math Imag. Vis., Vol. 47, 2013, pp. 179-209.
- [5] F.A. Gonzalez, E. Romero, "Biomedical image analysis and machine learning technologies", Med. Inform. Sci. Ref. Hershey, 2010.
- [6] M. J. Fadili, J. L. Starck, "Curvelets and Ridgelets", Springer, Computational Complexity, 2012, 754-773.
- [7] E. J. Candes, "What is a Curvelet?", AMS, Vol. 50, No. 11, 2003, pp.1402-1403.
- [8] K. P. Soman, K. I. Ramachandran, N. G. Resmi, "Insight into wavelets from theory to practice", PHI Learning Private limited, New delhi, 2010, pp. 349-391.
- [9] X. Cai, R. Chan, Z. Shen, "A framelet-based image inpainting algorithm", Applied and Computational Harmonic Analysis, Vol. 24, 2008, pp. 131-149.
- [10] T. Lindeberg, "Scale-space theory in computer vision", Dordrecht, The Netherlands: Kluwer Academic, 1997.
- [11] J. Staal, M. D. Ambramo, M. Niemeijer, M.A. Viergever, B. V. Ginneken, "Ridge based vessel segmentation in color Images of the retina", IEEE Trans. Medical Imaging, Vol. 23, 2004, pp. 501-509.
- [12] I. Daubechies, "Ten lectures on wavelets", SIAM, CBMS-NSF Regional Conference Series in Applied Mathematics, 1992.
- [13] E. Aboufadel, S. Schlicker, "Discovering wavelets", A Wiley-Interscience Publication, 1999.
- [14] B. Dong, A. Chien, Z. Shen, "Frame based segmentation for medical image", Communications in Mathematical Sciences, Vol. 32, No. 4, 2010, pp. 1724-1739.
- [15] Y. Li, J. Kim, "An unconditionally stable numerical method for bimodal image segmentation", Applied Mathematics and Computation, Vol. 219, 2012, pp. 3083-3090.
- [16] L. Donoho, M. Johnstone, "Adapting to Unknown Smoothness via Wavelet Shrinkage", Journal of the American Statistical Association, Vol. 90, No. 432, 1995, pp. 1200-1244.
- [17] L. M. J. Florack, "Image structure", Dordrecht, The Netherlands: Kluwer Academic, 1997.
- [18] E. Candes, L. Demanet, D. Donoho, L. Ying, "Fast Discrete Curvelet Transforms", SIAM, Multiscale Model. Simul., Vol. 5, Is. 3, 2006, pp. 861-899.

[19] R. Jain, R. Kasturi, B. G. Schunck, "*Machine vision*", McGraw-Hill, 1995.

BIOGRAPHY

Nasser Aghazadeh is an associate professor at Azarbaijan Shahid Madani University, Tabriz, Iran. He obtained his M.Sc. degree in Applied Mathematics (Numerical Analysis) from "Iran University of Science & Technology" and he obtained his PhD degree in Applied Mathematics in the same place under supervision of Professor Khosrow Maleknejad on June 2007. His current research interests include numerical analysis, mathematical image processing, wavelets, etc. He is a member of "Research Group of Processing and Communication" Azarbaijan Shahid Madani University, Tabriz, Iran. He can be contacted at aghazadeh@azaruniv.ac.ir.

Ladan Sharafyan Cigaroudy obtained her M.Sc. degree in Applied Mathematics from Tarbiat Modaress University of Tehran, Iran, in 2005. She is currently a PhD student in the Department of Applied Mathematics at Azarbaijan Shahid Madani University, Tabriz, Iran. She can be contacted at sharafyan@azaruniv.ac.ir.